Categorizing resonances $X(1835)$, $X(2120)$, and $X(2370)$ in the pseudoscalar meson family

Jie-Sheng Yu,[1,2] Zhi-Feng Sun,[1,2] Xiang Liu,[1,2,*,†] and Qiang Zhao[3,4,‡]

[1]*School of Physical Science and Technology, Lanzhou University, Lanzhou 730000, China*
[2]*Research Center for Hadron and CSR Physics, Lanzhou University and Institute of Modern Physics of CAS, Lanzhou 730000, China*
[3]*Institute of High Energy Physics, Chinese Academy of Sciences, Beijing 100049, China*
[4]*Theoretical Physics Center for Science Facilities, CAS, Beijing 100049, China*

(Received 28 April 2011; published 1 June 2011)

Inspired by the newly observed three resonances $X(1835)$, $X(2120)$, and $X(2370)$, in this work we systematically study the two-body strong decays and double pion decays of $\eta(1295)/\eta(1475)$, $\eta(1760)/X(1835)$, and $X(2120)/X(2370)$ by categorizing $\eta(1295)/\eta(1475)$, $\eta(1760)/X(1835)$, $X(2120)$, and $X(2370)$ as the radial excitations of $\eta(548)/\eta'(958)$. Our numerical results indicate the followings: (1) The obtained theoretical strong decay widths of three pseudoscalar states $\eta(1295)$, $\eta(1475)$, and $\eta(1760)$ are consistent with the experimental measurements; (2) $X(1835)$ could be the second radial excitation of $\eta'(958)$; (3) $X(2120)$ and $X(2370)$ can be explained as the third and fourth radial excitations of $\eta(548)/\eta'(958)$, respectively. The predicted two-body decay patterns of $\eta(1295)/\eta(1475)$, $\eta(1760)/X(1835)$, and $X(2120)/X(2370)$ and their double pion decays should be useful for further testing the conventional meson assignment to $\eta(1295)/\eta(1475)$, $\eta(1760)/X(1835)$, $X(2120)$, and $X(2370)$.

DOI: 10.1103/PhysRevD.83.114007 PACS numbers: 14.40.Be, 12.38.Lg, 13.25.Jx

I. INTRODUCTION

Very recently, the BES-III Collaboration reported the observation of several resonant structures in the $\eta'\pi^+\pi^-$ invariant mass spectrum in $J/\psi \to \gamma\eta'\pi^+\pi^-$ [1]. Among these resonant structures, $X(1835)$ that was first observed by the BES-II Collaboration [2], was confirmed with mass and width of $M_{X(1835)} = 1836.5 \pm 3.0(\text{stat.})^{+5.6}_{-2.1}(\text{syst.})$ MeV, and $\Gamma_{X(1835)} = 190 \pm 9(\text{stat.})^{+38}_{-36}(\text{syst.})$ MeV, respectively. The BES-II determinations of the $X(1835)$ resonance parameters are $M = 1833.7 \pm 6.5(\text{stat.}) \pm 2.7(\text{syst.})$ MeV and $\Gamma = 67.7 \pm 20.3(\text{stat.}) \pm 7.7(\text{syst.})$ MeV, with $J^{PC} = 0^{-+}$. In contrast with the BES-III result, it shows that the newly measured width is larger than that from BES-II.

Apart from the $X(1835)$, the observation of another two resonant structures initiate a lot of interests here, i.e.,

$$M_{X(2120)} = 2122.4 \pm 6.7(\text{stat.})^{+4.7}_{-2.7}(\text{syst.}) \text{ MeV},$$
$$\Gamma_{X(2120)} = 83 \pm 16(\text{stat.})^{+31}_{-11}(\text{syst.}) \text{ MeV},$$
$$M_{X(2370)} = 2376.3 \pm 8.7(\text{stat.})^{+3.2}_{-4.3}(\text{syst.}) \text{ MeV},$$
$$\Gamma_{X(2370)} = 83 \pm 17(\text{stat.})^{+44}_{-6}(\text{syst.}) \text{ MeV},$$

where we refer to these two new structures by the names $X(2120)$ and $X(2370)$ in this work.

In 2005, when $X(1835)$ was first announced by the BES-II Collaboration, it immediately stimulated tremendous interest in its internal structure. In particular, its appearance in $\eta'\pi^+\pi^-$ instead of $\eta\pi^+\pi^-$ has initiated various interpretations based on exotic configurations. Taking into account the new observation of the $X(2120)$ and $X(2370)$ by BES-III, it could be a great opportunity for us to gain some deep insights into the isoscalar pseudoscalar meson spectrum. To proceed, we first give a brief review of the studies of the $X(1835)$ in the literature. We will then propose a classification scheme to combining the $X(2120)$ and $X(2370)$ with the existing pseudoscalar mesons in the quark pair creation (QPC) model.

In Ref. [3], $X(1835)$ was explained as the lowest pseudoscalar glueball state due to the instanton mechanism of partial $U(1)_A$ symmetry restoration. For further explanation of why the mass of $X(1835)$ is lower than the prediction of the quenched lattice QCD and QCD sum rules (QCDSR), an η_c-glueball mixing mechanism was proposed [4]. Later, the authors of Ref. [5] studied the QCD anomaly contribution to $X(1835)$ using the QCDSR, and obtained a sizable matrix element $\langle 0|G\tilde{G}|G_P\rangle$ for $X(1835)$. It shows that $X(1835)$ could be explained as a pseudoscalar state with a large gluon content. In Ref. [6], a further study of $X(1835)$ as a pseudoscalar glueball was performed by estimating the decay rates of $X(1835) \to VV$, γV, $\gamma\gamma$ and cross sections of $\gamma\gamma \to X(1835) \to f$ and $h_1 + h_2 \to X(1835) + \cdots$ by an effective Lagrangian approach. A 0^{-+} trigluon glueball with mass range 1.9–2.7 GeV was also investigated within a baryonium-gluonium mixing picture using the QCDSR [7].

It is worth mentioning that before the observation of $X(1835)$, the BES-II Collaboration once reported a $p\bar{p}$ subthreshold enhancement $X(1860)$ in the $J/\psi \to \gamma p\bar{p}$ decay [8]. This observation has also stimulated broad studies of the nature of this enhancement among which the $p\bar{p}$ baryonium appears to be attractive [9–12]. The new data from the BES-III Collaboration also confirmed the $X(1860)$ signal in $\psi' \to \pi^+\pi^- J/\psi(J/\psi \to \gamma p\bar{p})$ [13].

*Corresponding author.
†xiangliu@lzu.edu.cn
‡zhaoq@ihep.ac.cn

Later, the CLEO Collaboration also reported the observation of $X(1860)$ [14] as an independent confirmation of this enhancement. Combining the $X(1860)$ signal with the later observed $X(1835)$ by BES-II, it was conjectured that these two structures might be originated from the same resonant state. Ding and Yan proposed that $X(1835)$ could be treated as a baryonium with a sizable gluon content. This would explain why $X(1835)$ was produced in the J/ψ radiative decays and with large couplings to $p\bar{p}$, $\eta'\pi\pi$ [15–17]. Calculations by the QCDSR [18] and large-N_c QCD [19] seemed to support that $X(1835)$ contained a baryonium component. A study based on the conventional $N\bar{N}$ potential model [20] suggested that $X(1835)$ could be a broad and weakly bound state $N\bar{N}_S(1870)$ in the $^{11}S_0$ wave. However, the calculations of the strong and electromagnetic decays of $X(1835)$ under the baryonium assumption obtained a rather small width for $X(1835) \to \eta'\pi^+\pi^-$ [21].

Apart from those proposed explanations for $X(1835)$ as an exotic state, efforts have also been made to understand $X(1835)$ from the point of view of a conventional $q\bar{q}$ state. Huang and Zhu treated $X(1835)$ as the second radial excitation of $\eta'(958)$ and discussed the strong decay behavior by the effective Lagrangian approach [22]. In Ref. [23], several two-body strong decays of $X(1835)$ associated with $\eta(1760)$ were studied by the QPC model, where $X(1835)$ is assigned as the $n^{2s+1}L_J = 3^1S_0$ state.

Although great efforts have been made in the literature, the properties of $X(1835)$ still remain unclear at present. This situation may be improved by the BES-III observations of $X(2120)$ and $X(2370)$ associated with $X(1835)$ in the $\eta'\pi^+\pi^-$ invariant mass spectrum. Nevertheless, the upgraded experimental information may allow us to have an overall view of the pseudoscalar meson spectrum, which has not been systematically addressed before.

To proceed, we organize the paper as follows. After the Introduction, we propose a quark model scheme to organize the so-far observed pseudoscalar mesons based on a qualitative analysis of the pseudoscalar mass spectrum. In Sec. III, the QPC model for the study of the strong decays of $\eta(1295)$, $\eta(1475)$, $\eta(1760)$, $X(1835)$, $X(2120)$, and $X(2370)$ in our categorizing scheme is summarized. In Sec. IV, the numerical results are presented and compared with the experimental data. Discussion and conclusion are given in Sec. V.

II. THE CATEGORIZING SCHEME FOR THE PSEUDOSCALAR MESON SPECTRUM

In the particle data group (PDG) [24], six isoscalar pseudoscalar states, $\eta(548)$, $\eta'(958)$, $\eta(1295)$, $\eta(1405)$, $\eta(1475)$, $\eta(1760)$, and $\eta(2225)$, are listed as observed states. Among these states, $\eta(548)$ and $\eta'(958)$ are well established as the ground states of the 0^- nonet associated with π^0, $\pi^\pm$, $K^\pm$, K^0, and $\bar{K}^0$. Such a quark model scenario should be a good starting point for classifying the observed higher pseudoscalar states as radial excitations of the ground states (see Table I).

It is well established that $\pi^{\pm,0}$, $K^{\pm,0}$, $\bar{K}^0$, $\eta(548)$, and $\eta'(958)$ belong to the ground state pseudoscalar nonet. It is also recognizable that $\pi(1300)$, $K(1460)$, $\eta(1295)$, and $\eta(1475)$ make the first radial excitation states of 0^- mesons [25]. There have been broad discussions about the nature of $\eta(1405)$. For instance, a recent review of this state can be found in Refs. [24,26,27]. In most theoretical studies [28–33], the decay patterns of $\eta(1405)$ indicate it as being a possible candidate of 0^{-+} glueball with the mass consistent with the prediction of the flux tube model [34]. In any case, if one leaves $\eta(1405)$ as a pseudoscalar glueball and to be investigated separately, it is interesting to recognize a pseudoscalar nonet of the second radial excitations formed by $\pi(1800)$, $K(1830)$, $\eta(1760)$, and $X(1835)$. Note that $\eta(1760)$ was observed in the invariant mass spectra of $\omega\omega$ [35] and $\rho\rho$ [36]. It makes a natural assignment of $\eta(1760)$ as the second radial excitation of $\eta(548)$. In contrast, $X(1835)$ strongly couples to $\eta'\pi^+\pi^-$ instead of $\eta\pi^+\pi^-$. This makes it a reasonable partner of $\eta(1760)$ as the second radial excitation of $\eta'(958)$ [22].

Since $X(2120)$ and $X(2370)$ associated with $X(1835)$ were observed in the $\eta'\pi\pi$ mass spectrum, we naturally deduce that the newly observed $X(2120)$ and $X(2370)$ could be categorized as the radial excitation states in the $\eta - \eta'$ family. There exist several possible assignments to $X(2120)$ and $X(2370)$ due to lack of further experimental information: (1) $X(2120)$ is the third radial excitation of $\eta(548)$ or $\eta'(958)$; (2) $X(2370)$ is the fourth radial excitation of $\eta(548)$ or $\eta'(958)$; (3) $X(2120)$ and $X(2370)$ are the third radial excitations of $\eta(548)$ and $\eta'(958)$, respectively.

The above categorizing can also be understood by examining the mass spectrum. In Fig. 1, we present the mass spectrum of all of these states with their mass gaps indicated explicitly by $\Delta_1^{(\prime)}$, $\Delta_2^{(\prime)}$, and Σ_i with $(i = 1, 2, 3)$. The qualitative relations, $\Delta_2 < \Delta_1$, $\Delta_2' < \Delta_1'$, and $\Sigma_3 < \Sigma_2 < \Sigma_1$, are consistent with the expectations of the

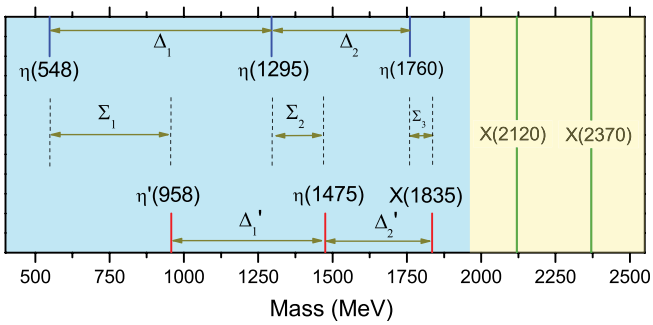

FIG. 1 (color online). A summary of the isoscalar pseudoscalar states assuming $X(2120)$ and $X(2370)$ as pseudoscalar states. Here, all data are taken from PDG [24] and the BES observations [1,2].

constituent quark model. It supports the assignment to $X(1835)$ as the second radial excitation of $\eta'(958)$.

Following the above relations, we can apply $\Delta_j < \Delta_i$ and $\Delta'_j < \Delta'_i$ with $(j > i)$ as a criteria to distinguish the different assignments to $X(2120)$ and $X(2370)$. $X(2120)$ as the third radial excitation of $\eta(548)$, or $\eta'(958)$ can result in the mass gap between $X(2120)$, and $\eta(1760)(X(1835))$ is smaller than the corresponding $\Delta_2(\Delta'_2)$. $X(2370)$ as the fourth radial excitation of $\eta(548)$ is suitable since the mass gap between $X(2370)$ and $X(2120)$ is smaller than that between $X(2120)$ and $\eta(1760)$. Additionally, $X(2370)$ could be as the fourth radial excitation of $\eta'(958)$, which will be discussed later.

The above assignments of $X(1835)$, $X(2120)$, and $X(2370)$ seem to be consistent with the analysis of Regge trajectories [37]. This is a valuable approach to provide quantitative estimate of hadron masses with the same quantum number. In Fig. 2, we plot the 0^{-+} trajectory on the plane of (n, M^2) adopting the relation $M^2 = M_0^2 + (n-1)\mu^2$ from Ref. [38], where M_0 is the ground state mass, n the radial quantum number, and μ^2 the slope parameter of the trajectory. It shows that $X(1835)$, $X(2120)$, and $X(2370)$ can be well accommodated into the trajectory.

Our assignment to $X(2370)$ and $X(2120)$ here is different from that suggested in Ref. [39], where $X(2120)$ and $X(2370)$ are assumed as the third radial excitations of $\eta(548)$ and $\eta'(958)$, respectively. In Ref. [39], it was concluded that $X(2120)$ and $X(2370)$ cannot be understood as the third radial excitations of $\eta(548)$ and $\eta'(958)$, while $X(2370)$ is probably a mixture of $\eta'(4^1S_0)$ and glueball. In this work, we expect that a systematic study of the two-body and double pion strong decays of all these states would provide useful information for our understanding of the η and η' spectrum.

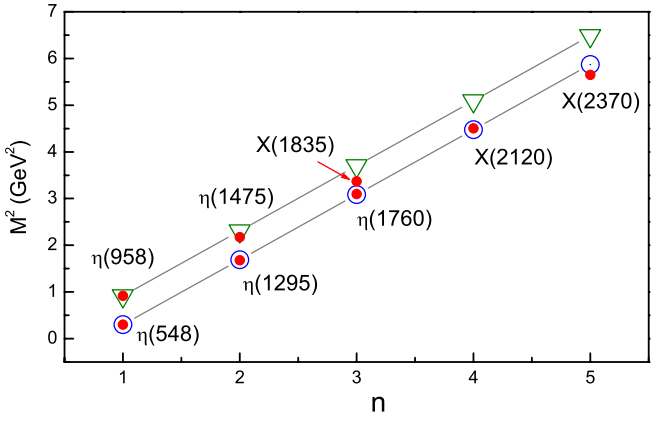

FIG. 2 (color online). The Regge trajectories for the η/η' mass spectrum with $M^2 = M_0^2 + (n-1)\mu^2$ ($\mu^2 = 1.39$ GeV) [38]. The η and η' trajectories are marked by "⊙" and "▽," respectively. The red points are experimental data from the PDG [24].

III. TWO-BODY AND THREE-BODY STRONG DECAYS

A. Quark pair creation model

In the following, we give a brief review of the QPC model (also known as the $^3P_0$ model) adopted in this work for the study of the strong decays of the states in the $\eta - \eta'$ family. Early developments of this method can be found in the literature [40–46]. It has also been broadly applied to the study of hadron properties related to recent progresses on the hadron spectroscopy [23,47–62].

In the QPC model, a transition operator T is introduced to describe a quark-antiquark pair creation from the vacuum

$$T = -3\gamma \sum_m \langle 1m; 1-m|00\rangle \int d\mathbf{k}_3 d\mathbf{k}_4 \delta^3(\mathbf{k}_3 + \mathbf{k}_4) \times \mathcal{Y}_{1m}\left(\frac{\mathbf{k}_3 - \mathbf{k}_4}{2}\right)\chi^{34}_{1,-m}\varphi_0^{34}\omega_0^{34} d^\dagger_{3i}(\mathbf{k}_3) b^\dagger_{4j}(\mathbf{k}_4), \quad (1)$$

where the dimensionless parameter γ denotes the creation strength of a quark-antiquark pair with quantum number $J^{PC} = 0^{++}$. i and j are the $SU(3)$ color indices of the created quark and antiquark. $\varphi_0^{34} = (u\bar{u} + d\bar{d} + s\bar{s})/\sqrt{3}$ and $\omega_0^{34} = \frac{1}{\sqrt{3}}\delta_{\alpha_3\alpha_4}(\alpha = 1, 2, 3)$ correspond to flavor and color singlets, respectively. $\chi^{34}_{1,-m}$ denotes a triplet state of spin. $\mathcal{Y}_{\ell m}(\mathbf{k}) \equiv |\mathbf{k}|^\ell Y_{\ell m}(\theta_k, \phi_k)$ is the ℓth solid harmonic polynomial. The schematic diagrams in Fig. 3 illustrate the decay transitions via the quark pair creation process. Note that the right diagram in Fig. 3 is valid only when the quark components in mesons A, B, and C are the same as each other.

The expression of decay width in the QPC model is written as

$$\Gamma = \pi^2 \frac{|\mathbf{K}|}{M_A^2} \sum_{JL} |\mathcal{M}^{JL}|^2, \quad (2)$$

where $\mathcal{M}^{JL}$ is the partial wave amplitude and related to the helicity amplitude $\mathcal{M}^{M_{J_A} M_{J_B} M_{J_C}}$ according to the Jacob-Wick formula [63]. The helicity amplitude $\mathcal{M}^{M_{J_A} M_{J_B} M_{J_C}}$ is obtained by the transition amplitude

$$\langle BC|T|A\rangle = \delta^3(\mathbf{K}_B + \mathbf{K}_C - \mathbf{K}_A)\mathcal{M}^{M_{J_A} M_{J_B} M_{J_C}}. \quad (3)$$

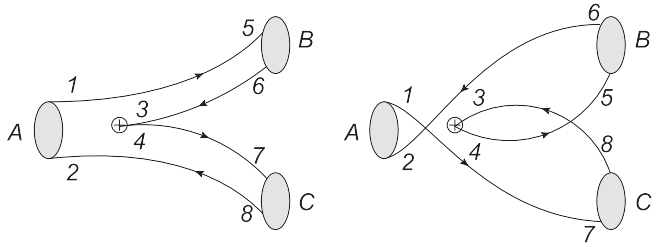

FIG. 3. The quark level diagrams describing meson decay in QPC model.

A detailed review of the QPC model and calculation of the transition amplitude $\langle BC|T|A\rangle$ have been given in Ref. [62], where the simple harmonic oscillator (SHO) wave function is applied to describe the meson spatial wave function

$$\Psi_{nLM}(\mathbf{k}) = \mathcal{N}_{nL}\exp\left(-\frac{R^2\mathbf{k}^2}{2}\right)\mathcal{Y}_{LM}(\mathbf{k})\mathcal{P}(\mathbf{k}^2), \qquad (4)$$

where $\mathcal{P}(\mathbf{k}^2)$ is a polynomial in terms of $\mathbf{k}^2$, the relative momentum between the quark and the antiquark within a meson, and $\mathcal{N}_{nL}$ represents the normalization coefficient.

B. Strong decay behavior

Before presenting the calculation results for the strong decays of $\eta(1295)$, $\eta(1440)$, $\eta(1760)$, $X(1835)$, $X(2120)$, $X(2370)$, we briefly introduce the mixing scheme of the $\eta - \eta'$ family. In the $SU(3)$ quark model, the physical states $\eta(nS)$ and $\eta'(nS)$ with the same radial excitation quantum number could be the mixtures of $\eta_q(nS)$ and $\eta_s(nS)$ in the flavor basis

$$\begin{pmatrix}\eta(nS)\\ \eta'(nS)\end{pmatrix} = \begin{pmatrix}\cos\theta_n & -\sin\theta_n\\ \sin\theta_n & \cos\theta_n\end{pmatrix}\begin{pmatrix}\eta_q(nS)\\ \eta_s(nS)\end{pmatrix}, \qquad (5)$$

where $\eta_q(nS)$ and $\eta_s(nS)$ are the flavor wave functions $|\eta_q(nS)\rangle = \frac{1}{\sqrt{2}}(|u\bar{u}\rangle + |d\bar{d}\rangle)$ and $|\eta_s(nS)\rangle = |s\bar{s}\rangle$, respectively. For instance, $\eta(548)/\eta'(958)$ are the ground states with $n = 1$, for which the commonly adopted mixing angle is $\theta_1 = (39.3 \pm 1.0)°$ [64]. For the first radial excitations, $\eta(1295)$ and $\eta(1475)$ are organized as the physical states with mixing angle θ_2. For $\eta(1760)/X(1835)$ and $X(2120)/X(2370)$ to be discussed in the following subsections, mixing angles θ_3, θ_4, and θ_5 are introduced, respectively. In contrast with the better determined mixing angle θ_1, information about other mixing angles θ_α ($\alpha = 2, 3, 4, 5$) is still absent. We expect that the θ_α-dependence of the resonance decay widths may provide some constraints on the mixing angles.

TABLE I. The pseudoscalar nonet.

$1S$	$2S$	$3S$	$4S$	$5S$
η, η'	$\eta(1295)$	$\eta(1760)$	$X(2120)$	$X(2370)$
	$\eta(1475)$	$X(1835)$		
$K(494)$	$K(1460)$	$K(1830)$		
π	$\pi(1300)$	$\pi(1800)$		

The two-body and double pion decay channels which are allowed by the conservation law are listed in Fig. 4 for $\eta(1295)$, $\eta(1440)$, $\eta(1760)$, $X(1835)$, $X(2120)$, and $X(2370)$. We assume that the double pion decay occurs through the intermediate scalar mesons, such as σ and $f_0(980)$.

By the QPC model, the general expressions of the partial wave amplitudes for the strong decays of $\eta(1295)/\eta(1440)$, $\eta(1760)/X(1835)$, $X(2120)/X(2370)$ are obtained and listed in Table II. $\Xi_{ij}^{k\ell}(nS)$ ($\Xi = \mathcal{I}, \mathcal{U}, \mathcal{Q}, \mathcal{G}$) is extracted from the spatial integral, which describes the overlap of the initial pseudoscalar meson

TABLE II. The general expressions of the partial wave amplitudes for the strong decays of $\eta(1295)/\eta(1475)$, $\eta(1760)/X(1835)$, and $X(2120)/X(2380)$. Here, $\mathcal{F}$ is the relevant flavor matrix element. Because of the complication of the concrete expressions of $\mathcal{I}_{ij}^{k\ell}(nS)$ and $\mathcal{Q}_{ij}^{k\ell}(nS)$, the detailed formulas of $\mathcal{I}_{ij}^{k\ell}(nS)$ and $\mathcal{Q}_{ij}^{k\ell}(nS)$ are not given in this work. E_β ($\beta = A, B, C$) are the energies of the initial and final states.

Decay modes	Partial wave amplitude
$0^- \to 0^- + 0^+$	$\mathcal{M}^{00} = \frac{\sqrt{2}}{3}\mathcal{F}\sqrt{E_AE_BE_C}\gamma[\mathcal{I}_{0-1}^{0-1}(nS) + \mathcal{I}_{00}^{00}(nS) + \mathcal{I}_{01}^{01}(nS)]$
$0^- \to 1^- + 1^+(^1P_1)$	$\mathcal{M}^{00} = \frac{\sqrt{2}}{3}\mathcal{F}\sqrt{E_AE_BE_C}\gamma[\mathcal{I}_{0-1}^{0-1}(nS) + \mathcal{I}_{00}^{00}(nS) + \mathcal{I}_{01}^{01}(nS)]$
$0^- \to 1^- + 1^+(^3P_1)$	$\mathcal{M}^{00} = \frac{2}{3}\mathcal{F}\sqrt{E_AE_BE_C}\gamma[\mathcal{I}_{0-1}^{0-1}(nS) + \mathcal{I}_{00}^{00}(nS) + \mathcal{I}_{01}^{01}(nS)]$
$0^- \to 0^- + 1^-$	$\mathcal{M}^{11} = \sqrt{\frac{2}{3}}\mathcal{F}\sqrt{E_AE_BE_C}\gamma\mathcal{Q}_{00}^{00}(nS)$
$0^- \to 0^+ + 1^+(^1P_1)$	$\mathcal{M}^{11} = -\frac{\sqrt{2}}{3}\mathcal{F}\sqrt{E_AE_BE_C}\gamma[\mathcal{U}_{-10}^{0-1}(nS) + \mathcal{U}_{00}^{00}(nS) + \mathcal{U}_{10}^{01}(nS)]$
$0^- \to 0^+ + 1^+(^3P_1)$	$\mathcal{M}^{11} = -\mathcal{F}\frac{1}{3}\sqrt{E_AE_BE_C}\gamma[\mathcal{U}_{0-1}^{0-1}(nS) + \mathcal{U}_{-11}^{00}(nS) + \mathcal{U}_{1-1}^{00}(nS) + \mathcal{U}_{01}^{01}(nS)]$
$0^- \to 1^+(^1P_1) + 1^+(^1P_1)$	$^*\mathcal{M}^{11} = 0$
$0^- \to 1^- + 1^-$	$\mathcal{M}^{11} = -\frac{2}{\sqrt{3}}\mathcal{F}\sqrt{E_AE_BE_C}\gamma\mathcal{Q}_{00}^{00}(nS)$
$0^- \to 0^- + 2^+$	$\mathcal{M}^{22} = \frac{1}{3}\mathcal{F}\sqrt{E_AE_BE_C}\gamma[\mathcal{I}_{0-1}^{0-1}(nS) - 2\mathcal{I}_{00}^{00}(nS) + \mathcal{I}_{01}^{01}(nS)]$
$0^- \to 0^+ + 2^-(^1D_2)$	$\mathcal{M}^{22} = \frac{\sqrt{2}}{3}\mathcal{F}\sqrt{E_AE_BE_C}\gamma[\mathcal{G}_{-10}^{0-1}(nS) + \mathcal{G}_{00}^{00}(nS) + \mathcal{G}_{10}^{01}(nS)]$
$0^- \to 0^+ + 2^-(^3D_2)$	$\mathcal{M}^{22} = \frac{1}{3}\mathcal{F}\sqrt{E_AE_BE_C}\gamma[\mathcal{G}_{0-1}^{0-1}(nS) + \mathcal{G}_{-11}^{00}(nS) + \mathcal{G}_{1-1}^{00}(nS) + \mathcal{G}_{01}^{01}(nS)]$
$0^- \to 1^- + 2^+$	$\mathcal{M}^{22} = -\frac{1}{\sqrt{6}}\mathcal{F}\sqrt{E_AE_BE_C}\gamma[\mathcal{I}_{0-1}^{0-1}(nS) - 2\mathcal{I}_{00}^{00}(nS) + \mathcal{I}_{01}^{01}(nS)]$
$0^- \to 1^- + 1^+(^1P_1)$	$\mathcal{M}^{22} = \frac{1}{3}\mathcal{F}\sqrt{E_AE_BE_C}\gamma[\mathcal{I}_{0-1}^{0-1}(nS) - 2\mathcal{I}_{00}^{00}(nS) + \mathcal{I}_{01}^{01}(nS)]$
$0^- \to 1^- + 1^+(^3P_1)$	$\mathcal{M}^{22} = -\frac{1}{3\sqrt{2}}\mathcal{F}\sqrt{E_AE_BE_C}\gamma[\mathcal{I}_{0-1}^{0-1}(nS) - 2\mathcal{I}_{00}^{00}(nS) + \mathcal{I}_{01}^{01}(nS)]$

with the radial quantum number n and the created pair within the two final mesons. Here, the SHO wave function $\Psi_{n\ell m}(\mathbf{k}) = R_{n\ell m}(R, \mathbf{k})\mathcal{Y}_{n\ell m}(\mathbf{k})$ is introduced in the calculation of the spatial integrals.

The input parameters, which include the R values in the SHO wave functions, flavor wave functions, masses, and the creation strength of a quark-antiquark pair from vacuum, are collected in Table III.

TABLE III. The input parameters for the strong decays of $\eta(1295)/\eta(1440)$, $\eta(1760)/X(1835)$, and $X(2120)/X(2370)$. Other common parameters, quark masses $m_u = m_d = 220$ MeV and $m_s = 419$ MeV, are fixed. The strengths of $q\bar{q}$ and $s\bar{s}$ created from vacuum are $\gamma_q = 6.3$ and $\gamma_s = \gamma_q/\sqrt{3}$, respectively. The parameter R in the harmonic oscillator wave function is fitted by requiring reproduction of the realistic root mean square radius which is obtained by solving the Schrödinger equation with the potential in Ref. [54].

Particle	Mass (MeV)	Flavor wave function	J^{PC}	$n^{2s+1}L_J$	R (GeV^{-1}) [54]
η [64]	548	$\cos\theta_1(\frac{u\bar{u}+d\bar{d}}{\sqrt{2}}) - \sin\theta_1(s\bar{s})$, $\theta_1 = 39.3°$	0^{-+}	1^1S_0	2.106
σ [65,66]	600	$-\sin\varphi(s\bar{s}) + \cos\varphi(\frac{u\bar{u}+d\bar{d}}{\sqrt{2}})$, $\varphi = 140°$	0^{++}	1^3P_0	3.486
ρ [24]	775.49	$\rho^+ = u\bar{d}$, $\rho^- = \bar{u}d$, $\rho^0 = \frac{u\bar{u}-d\bar{d}}{\sqrt{2}}$	1^{--}	1^3S_1	3.571
ω	782.65	$\frac{u\bar{u}+d\bar{d}}{\sqrt{2}}$	1^{--}	1^3S_1	3.571
η' [64]	958	$\sin\theta_1(\frac{u\bar{u}+d\bar{d}}{\sqrt{2}}) + \cos\theta_1(s\bar{s})$, $\theta_1 = 39.3°$	0^{-+}	1^1S_0	2.106
$f_0(980)$ [65,66]	980	$\cos\varphi(s\bar{s}) + \sin\varphi(\frac{u\bar{u}+d\bar{d}}{\sqrt{2}})$, $\varphi = 140°$	0^{++}	1^3P_0	3.486
$a_0(980)$ [24]	984.7	$a_0^+ = u\bar{d}$, $a_0^- = \bar{u}d$, $a_0^0 = \frac{u\bar{u}-d\bar{d}}{\sqrt{2}}$	0^{++}	1^3P_0	3.846
$\phi(1020)$	1019.45	$s\bar{s}$	1^{--}	1^3S_1	2.778
$h_1(1170)$ [67]	1170	$0.997(\frac{u\bar{u}+d\bar{d}}{\sqrt{2}}) + 0.073(s\bar{s})$	1^{+-}	1^1P_1	3.704
$b_1(1235)$ [24]	1229.5	$b_1^+ = u\bar{d}$, $b_1^- = \bar{u}d$, $b_1^0 = \frac{u\bar{u}-d\bar{d}}{\sqrt{2}}$	1^{+-}	1^1P_1	3.704
$a_1(1260)$ [24]	1230	$a_1^+ = u\bar{d}$, $a_1^- = \bar{u}d$, $a_1^0 = \frac{u\bar{u}-d\bar{d}}{\sqrt{2}}$	1^{++}	1^3P_1	3.846
$f_2(1270)$ [68,69]	1275	$\frac{u\bar{u}+d\bar{d}}{\sqrt{2}}$	2^{++}	1^3P_2	3.846
$f_1(1285)$ [70]	1281.8	$\cos\epsilon(\frac{u\bar{u}+d\bar{d}}{\sqrt{2}}) - \sin\epsilon(s\bar{s})$, $\epsilon = 35.3°$	1^{++}	1^3P_1	3.486
$\eta(1295)$	1295	$\cos\theta_2(\frac{u\bar{u}+d\bar{d}}{\sqrt{2}}) - \sin\theta_2(s\bar{s})$, $\theta_2 = ?$	0^{-+}	2^1S_0	3.301
$\pi(1300)$ [24]	1300	$\pi^+ = u\bar{d}$, $\pi^- = \bar{u}d$, $\pi^0 = \frac{u\bar{u}-d\bar{d}}{\sqrt{2}}$	0^{-+}	2^1S_0	3.571
$a_2(1320)$ [24]	1318.3	$a_2^+ = u\bar{d}$, $a_2^- = \bar{u}d$, $a_2^0 = \frac{u\bar{u}-d\bar{d}}{\sqrt{2}}$	2^{++}	1^3P_2	3.846
$f_1(1420)$ [70]	1426.4	$\sin\epsilon(\frac{u\bar{u}+d\bar{d}}{\sqrt{2}}) + \cos\epsilon(s\bar{s})$, $\epsilon = 35.3°$	1^{++}	1^3P_1	3.486
$\omega(1420)$ [24]	1400–1450	$\frac{u\bar{u}+d\bar{d}}{\sqrt{2}}$	1^{--}	2^3S_1	4.167
$\rho(1450)$ [24]	1465	$\rho^+ = u\bar{d}$, $\rho^- = \bar{u}d$, $\rho^0 = \frac{u\bar{u}-d\bar{d}}{\sqrt{2}}$	1^{--}	2^3S_1	4.167
$\eta(1475)$	1475	$\sin\theta_2(\frac{u\bar{u}+d\bar{d}}{\sqrt{2}}) + \cos\theta_2(s\bar{s})$, $\theta_2 = ?$	0^{-+}	2^1S_0	3.301
$a_0(1450)$ [24]	1474	$a_0^+ = u\bar{d}$, $a_0^- = \bar{u}d$, $a_0^0 = \frac{u\bar{u}-d\bar{d}}{\sqrt{2}}$	0^{++}	2^3P_0	4.347
$f_2'(1525)$ [68,69]	1525	$s\bar{s}$	2^{++}	1^3P_2	3.125
$a_2(1700)$ [24]	1732	$a_2^+ = u\bar{d}$, $a_2^- = \bar{u}d$, $a_2^0 = \bar{a}_2^0 = \frac{u\bar{u}-d\bar{d}}{\sqrt{2}}$	2^{++}	2^3P_2	4.347
$\eta(1760)$	1756	$\cos\theta_3(\frac{u\bar{u}+d\bar{d}}{\sqrt{2}}) - \sin\theta_3(s\bar{s})$, $\theta_3 = ?$	0^{-+}	3^1S_0	3.869
$X(1835)$	1835	$\sin\theta_3(\frac{u\bar{u}+d\bar{d}}{\sqrt{3}}) + \cos\theta_3(s\bar{s})$, $\theta_3 = ?$	0^{-+}	3^1S_0	3.869
$X(2120)$	2120	$\cos\theta_4(\frac{u\bar{u}+d\bar{d}}{\sqrt{2}}) - \sin\theta_4(s\bar{s})$, $\theta_4 = ?$ $\sin\theta_4(\frac{u\bar{u}+d\bar{d}}{\sqrt{2}}) + \cos\theta_4(s\bar{s})$	0^{-+}	4^1S_0	?
$X(2370)$	2370	$\cos\theta_5(\frac{u\bar{u}+d\bar{d}}{\sqrt{3}}) - \sin\theta_5(s\bar{s})$, $\theta_5 = ?$ $\sin\theta_5(\frac{u\bar{u}+d\bar{d}}{\sqrt{2}}) + \cos\theta_5(s\bar{s})$	0^{-+}	5^1S_0	4.348
K [24]	493.68(497.61)	$K^+ = u\bar{s}$, $K^- = \bar{u}s$, $K^0 = d\bar{s}$, $\bar{K}^0 = \bar{d}s$	0^-	1^1S_0	2.174
K^* [24]	892(896)	$K^{*+} = u\bar{s}$, $K^{*-} = \bar{u}s$, $K^{*0} = d\bar{s}$, $\bar{K}^{*0} = \bar{d}s$	1^-	1^3S_1	3.125
$K_1(1270)$ [24]	1272	$K_1^+ = u\bar{s}$, $K_1^- = \bar{u}s$, $K_1^0 = d\bar{s}$, $\bar{K}_1^0 = \bar{d}s$	1^+	$\sin\theta\|1^3P_1\rangle + \cos\theta\|1^1P_1\rangle$	3.448
$K_1(1400)$ [24]	1403	$K_1^+ = u\bar{s}$, $K_1^- = \bar{u}s$, $K_1^0 = d\bar{s}$, $\bar{K}_1^0 = \bar{d}s$	1^+	$\cos\theta\|1^3P_1\rangle - \sin\theta\|1^1P_1\rangle$ $\theta = -34°$ [71]	3.448
$K^*(1410)$ [24]	1414	$K^{*+} = u\bar{s}$, $K^{*-} = \bar{u}s$, $K^{*0} = d\bar{s}$, $\bar{K}^{*0} = \bar{d}s$	1^-	2^3S_1	3.846
$K_0^*(1430)$	1425	$K_0^{*+} = u\bar{s}$, $K_0^{*-} = \bar{u}s$, $K_0^{*0} = d\bar{s}$, $\bar{K}_0^{*0} = \bar{d}s$	0^+	1^3P_0	3.448
$K_2^*(1430)$ [24]	1425.6(1432.4)	$K_2^{*+} = u\bar{s}$, $K_2^{*-} = \bar{u}s$, $K_2^{*0} = d\bar{s}$, $\bar{K}_2^{*0} = \bar{d}s$	2^+	1^3P_2	3.448
$K(1460)$ [24]	1460	$K^+ = u\bar{s}$, $K^- = \bar{u}s$, $K^0 = d\bar{s}$, $\bar{K}^0 = \bar{d}s$	0^-	2^1S_0	3.448
$K^*(1680)$ [24]	1717	$K^{*+} = u\bar{s}$, $K^{*-} = \bar{u}s$, $K^{*0} = d\bar{s}$, $\bar{K}^{*0} = \bar{d}s$	1^-	3^3S_1	3.846

Modes	Channel	$\eta(1295)$	$\eta(1475)$	$\eta(1760)$	$X(1835)$	$X(2120)$	$X(2370)$
$0^- + 0^+$	$\pi a_0(980)$	■	■	■	■	■	■
	$\pi(1300)a_0(980)$						■
	$\pi a_0(1450)$			■	■	■	■
	$KK_0^*(1430)$					■	■
$1^- + 1^+$	$K^*K_1(1270)$						■
	$K^*K_1(1400)$						■
	$\omega(782)h_1(1170)$					■	■
	$\rho(770)b_1(1235)$					■	■
$0^- + 1^-$	KK^*		■	■	■	■	■
	$KK^*(1410)$					■	■
	$KK^*(1680)$						■
	$K(1460)K^*$						■
$0^+ + 1^+$	$a_0(980)a_1(1260)$						■
$1^- + 1^-$	K^*K^*				■	■	■
	$K^*K^*(1410)$						■
	$\rho(770)\rho(770)$			■	■	■	■
	$\rho(770)\rho(1450)$						■
	$\omega(782)\omega(782)$			■	■	■	■
	$\omega(782)\omega(1420)$						■
	$\phi\phi$					■	■
$1^+ + 1^+$	$h_1(1170)h_1(1170)$						■
$0^- + 2^+$	$\pi a_2(1320)$			■	■	■	■
	$\pi a_2(1700)$					■	■
	$\eta(548)f_2(1270)$				■	■	■
	$\eta(548)f_2'(1525)$					■	■
	$\eta'(958)f_2(1270)$						■
	$KK_2^*(1430)$					■	■
$1^- + 2^+$	$K^*K_2^*(1430)$						■
$0^- + 3^-$	$KK_3^*(1780)$						■
$0^- + S$	$\eta(548)\pi\pi$	■	■	■	■	■	■
	$\eta'(958)\pi\pi$	■	■	■	■	■	■
	$\eta(1295)\pi\pi$			■	■	■	■
	$\eta(1475)\pi\pi$			■	■	■	■
	$\eta(1760)\pi\pi$					■	■
$1^+ + S$	$f_1(1285)\pi\pi$			■	■	■	■
	$f_1(1420)\pi\pi$			■	■	■	■

FIG. 4 (color online). The two-body decays and double pion decays of $\eta(1295/\eta(1475)$, $\eta(1760)/X(1835)$, $X(2120)/X(2370)$. The double pion decays occur via the intermediate scalar mesons (S), such as $\sigma(600)$ and $f_0(980)$. Here, we use ■ to mark the allowed two-body decays and double pion decays of $\eta(1295/\eta(1475)$, $\eta(1760)/X(1835)$, $X(2120)/X(2370)$.

For estimating the double pion decay widths, we assume that the double pion decays listed in Fig. 4 occur through the intermediate scalar mesons σ and $f_0(980)$. The general expression of the double pion decay is [62]

$$\Gamma(X \to \eta + \mathcal{S} \to \eta + \pi\pi) = \sum_{\mathcal{S}=\sigma,f_0} \frac{1}{\pi} \int_{4m_\pi^2}^{(m_X - m_\eta)^2} dr \sqrt{r} \frac{\Gamma_{X\to\eta+\mathcal{S}}(r) \cdot \Gamma_{\mathcal{S}\to\pi\pi}(r)}{(r - m_{\mathcal{S}}^2)^2 + (m_{\mathcal{S}}\Gamma_{\mathcal{S}})^2}, \tag{6}$$

where X denotes any of the states in the $\eta - \eta'$ family. $\Gamma_{X\to\eta+\mathcal{S}}(r)$ is obtained in the QPC model. The effective Lagrangian describing the interaction of scalar state ($\mathcal{S} = \sigma$, $f_0(980)$) with two pions is written as

$$\mathcal{L}_{\mathcal{S}\pi\pi} = g_\sigma \sigma (2\pi^+\pi^- + \pi^0\pi^0), \tag{7}$$

where the coupling constants $g_\sigma = 2.60$–3.35 GeV and $g_{f_0} = 0.83$–1.30 GeV are determined by the total widths of σ and $f_0(980)$, i.e., $\Gamma_\sigma = 600$–1000 MeV and $\Gamma_{f_0} = 40$–100 MeV [24]. The decay amplitudes of $\mathcal{S} \to \pi\pi$ are

$$\Gamma_{\sigma\to\pi\pi} = \frac{g_\sigma^2 \lambda^2}{8\pi} \frac{p_1(r)}{r}, \tag{8}$$

where $p_1(r)$ denotes the three-vector momentum of the final state pion in the initial scalar rest frame.

In this work, we also discuss the sequential decay $X \to \pi + a_0(980) \to \eta\pi\pi$. The general expression of the decay width of $X \to \pi^0 + a_0(980)^0 \to \eta\pi^0\pi^0$ is similar to Eq. (6). It reads

$$\Gamma(X \to \pi^0 + a_0(980)^0 \to \eta\pi^0\pi^0) \approx \frac{1}{\pi} \int_{(m_{\pi^0}+m_\eta)^2}^{(m_X - m_{a^0})^2} dr \sqrt{r} \frac{\Gamma_{X\to\pi^0+a_0^0}(r) \cdot \Gamma_{a_0^0\to\pi^0\pi^0}(r)}{(r - m_{a_0}^2)^2 + (m_{a_0}\Gamma_{a_0})^2}, \tag{9}$$

where the decay width $\Gamma_{a_0^0\to\eta\pi^0} = (g_{a_0}^2/(8\pi r)) \times ((r - (m_\pi + m_\eta)(r - (m_\pi - m_\eta))/(2r^{1/2})$ with $g_{a_0} = 1.262$–2.524 GeV determined by the total decay width of $a_0(980)$ ($\Gamma_{a_0} = 50$–100 MeV). The final result of $\Gamma_{X\to\pi+a_0(980)\to\eta\pi\pi}$ includes the contributions from both $\eta\pi^+\pi^-$ and $\eta\pi^0\pi^0$.

IV. NUMERICAL RESULT

In this section, the numerical results for states $\eta(1295)$, $\eta(1475)$, $\eta(1760)$, $X(1835)$, $X(2120)$, and $X(2370)$, are presented by pairing them as the $\eta(nS)/\eta'(nS)$ partners. In the QPC model, the predicted partial widths will have dependence on the harmonic oscillator strength R. Thus, we will illustrate the partial widths in terms of R. By adopting the data for some of those measured channels, we can then examine the model predictions within a fixed range of R.

A. $\eta(1295)$ and $\eta(1475)$

The R-dependence of the total decay widths of $\eta(1295)/\eta(1475)$ are shown in Figs. 5(a) and 6(a), where their total decay widths are from the two-body and double pion decays. For $\eta(1295)$, there exists overlap between the theoretical result and experimental measurement with $R = 3.66$–3.69 GeV^{-1}, which is close to the value given in Ref. [54]. For $\eta(1475)$, the R range ($R = 3.91$–4.16 GeV^{-1}) for the overlap between the experimental and theoretical values is larger than that for

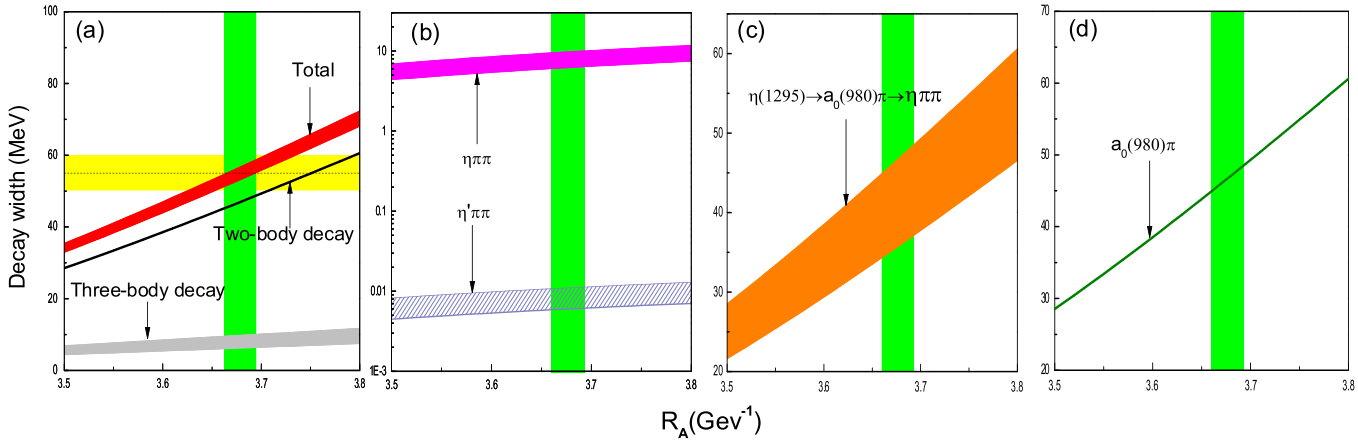

FIG. 5 (color online). The R dependence of the calculated total and partial widths of $\eta(1295)$. (a) The total decay width, two-body and three-body strong decay of $\eta(1295)$ in comparison with the experimental data (dashed line with yellow band). (b) The R dependence of the double pion decays of $\eta(1295)$ via the intermediate scalar states. (c) The decay width of $\eta(1295) \to a_0(980)\pi \to \eta\pi\pi$. (d) The partial two-body decay width of $\eta(1295)$. Here, the R range corresponding to the overlap between the total decay width and experimental data is marked by the green band.

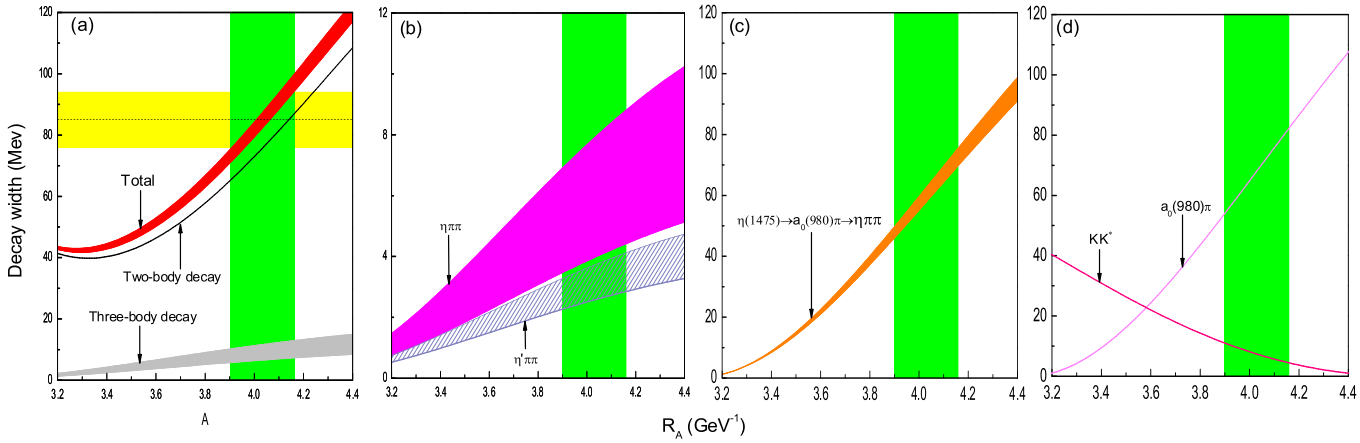

FIG. 6 (color online). The R dependence of the calculated total and partial widths of $\eta(1475)$. The partial widths presented in (a–d) are arranged in the same way as in Fig. 5.

$\eta(1295)$ as shown in Fig. 6(a). Furthermore, with such a R value for $\eta(1475)$, the partial widths of $\eta(1475) \to a_0(980)\pi$ and $K\bar{K}^* + c.c.$ are 55.1–82.3 MeV and 10.7–4.4 MeV, respectively. This seems to contradict the experimental data since the dominant decay channel of $\eta(1475)$ is $K\bar{K}\pi$, and $K\bar{K}\pi$ is possibly from the decay of $K\bar{K}^*(892) + c.c.$ Such inconsistency can be due to an unsuitable R range for $\eta(1475)$. If taking the same R range as that of $\eta(1295)$, we found the decay width of $\eta(1475) \to K\bar{K}^* + c.c.$ is comparable with that of $\eta(1475) \to a_0(980)\pi$, and the inconsistency mentioned above longer exists. The obtained total decay width of $\eta(1475)$ ($\Gamma = 53.5$–58.7 MeV) is smaller than the averaged value of the width of $\eta(1475)$ ($\Gamma = 85 \pm 9$ MeV) listed in PDG [24] and close to the central value ($\Gamma = 54$ MeV) given by the Mark-III Collaboration [72]. Regarding this situation, we expect that more precise experimental measurement of the $\eta(1475)$ resonance parameter, e.g., from BES-III, will help clarify this problem.

In Fig. 5(b), it shows that $\eta(1295)$ can dominantly decay into $\eta\pi\pi$ via the intermediate scalars. For $\eta(1475)$, the $\eta\pi\pi$ decay width is slightly larger than that of $\eta'\pi\pi$, as shown by Fig. 6(b). Since $\eta\pi$ is the dominant decay of $a_0(980)$ [24], the $a_0(980)\pi$ should be an important contributing channel in $\eta(1295)/\eta(1475) \to a_0(980)\pi \to \eta\pi\pi$. In Figs. 5(c) and 6(c), the R-dependences of the decay widths of $\eta(1295)/\eta(1475) \to a_0(980)\pi \to \eta\pi\pi$ are presented. We notice that the decay widths of $\eta(1295)/\eta(1475) \to \eta\pi\pi$ via intermediate $a_0(980)$ are comparable with those via intermediate scalar states σ and $f_0(980)$. It indicates that intermediate $a_0(980)$ contribution is important to the double pion decays of $\eta(1295)/\eta(1475)$, especially to $\eta(1475) \to \eta\pi\pi$. This can be tested by the experimental analysis of the $\eta\pi$ and $\pi\pi$ invariant mass spectra of $\eta(1295)/\eta(1475) \to \eta\pi\pi$.

B. $\eta(1760)$ and $X(1835)$

The calculation results for the $\eta(1760)$ and $X(1835)$ decays in terms of R are presented in Figs. 7 and 8,

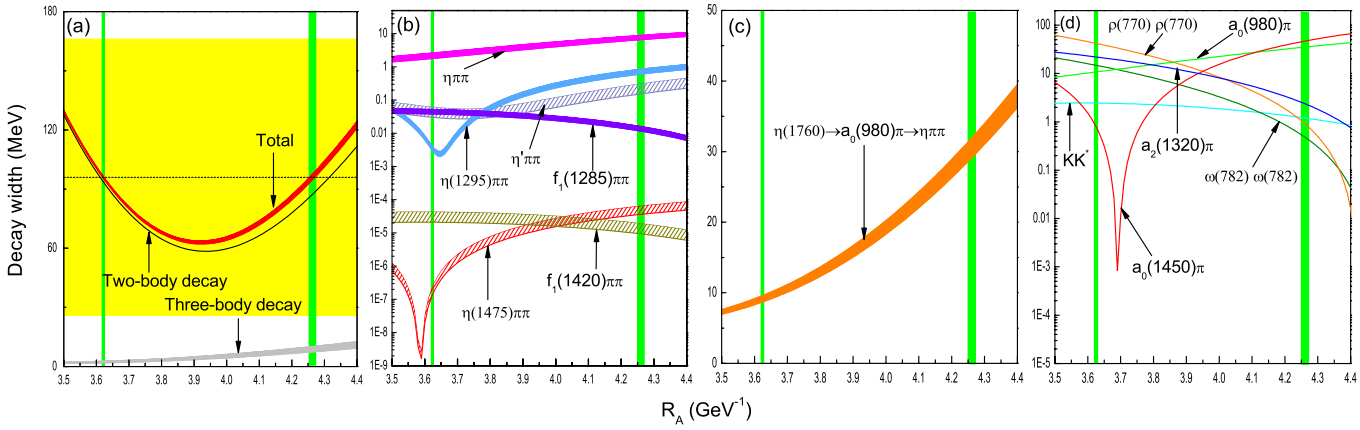

FIG. 7 (color online). The R dependence of the calculated total and partial widths of $\eta(1760)$. The partial widths presented in (a–d) are arranged in the same way as in Fig. 5.

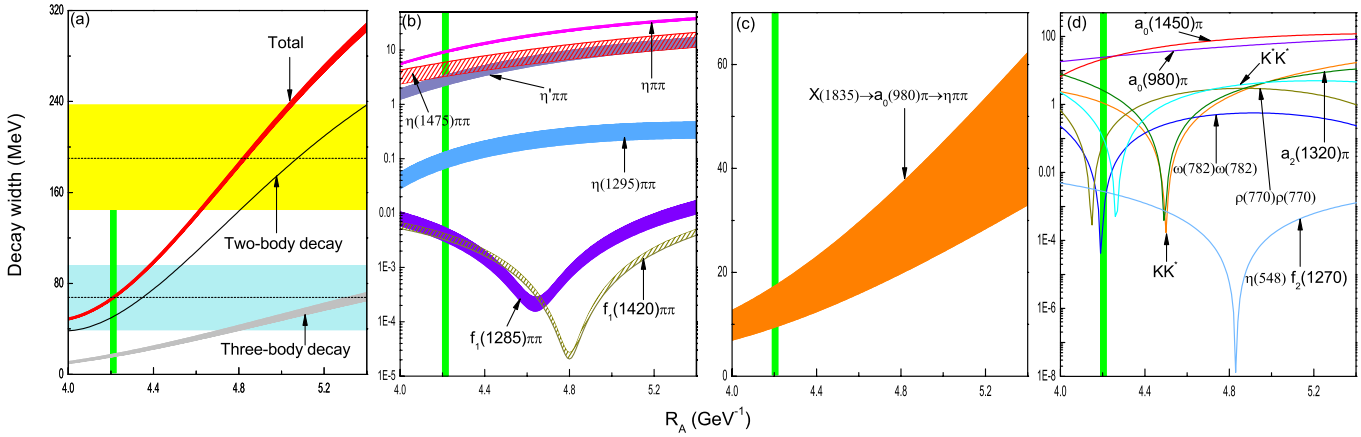

FIG. 8 (color online). The R dependence of the calculated total and partial widths of $X(1835)$. The partial widths presented in (a–d) are arranged in the same way as in Fig. 5. Here, dashed lines with yellow and blue bands are the BES-II [2] and BES-III [1] measurements of $X(1835)$ width, respectively.

respectively. As shown by Figs. 7(a) and 8(a), the total decay width of $\eta(1760)$ can fit the central value of the experimental width with $R = 3.62$–3.63 GeV^{-1} or $R = 4.26$–4.27 GeV^{-1}, due to large experimental uncertainties with the $\eta(1760)$ width.

To some extent, the behavior of partial decay width of $\eta(1760)$ with $R = 3.62$–3.63 GeV^{-1} [see Fig. 7(d)] can reflect the experimental observation of $\eta(1760)$ well. In this range, the partial widths are consistent with its signals observed in $J/\psi \to \gamma\omega\omega$ [35] and $\gamma\rho\rho$ [36]. The two-body partial decay widths of $\eta(1760)$ are given in Fig. 7(d), from which one sees that $\rho(770)\rho(770)$, $a_2(1320)\pi$, $\omega(782)\omega(782)$, and $a_0(980)\pi$ are the main decay channels for $\eta(1760)$,

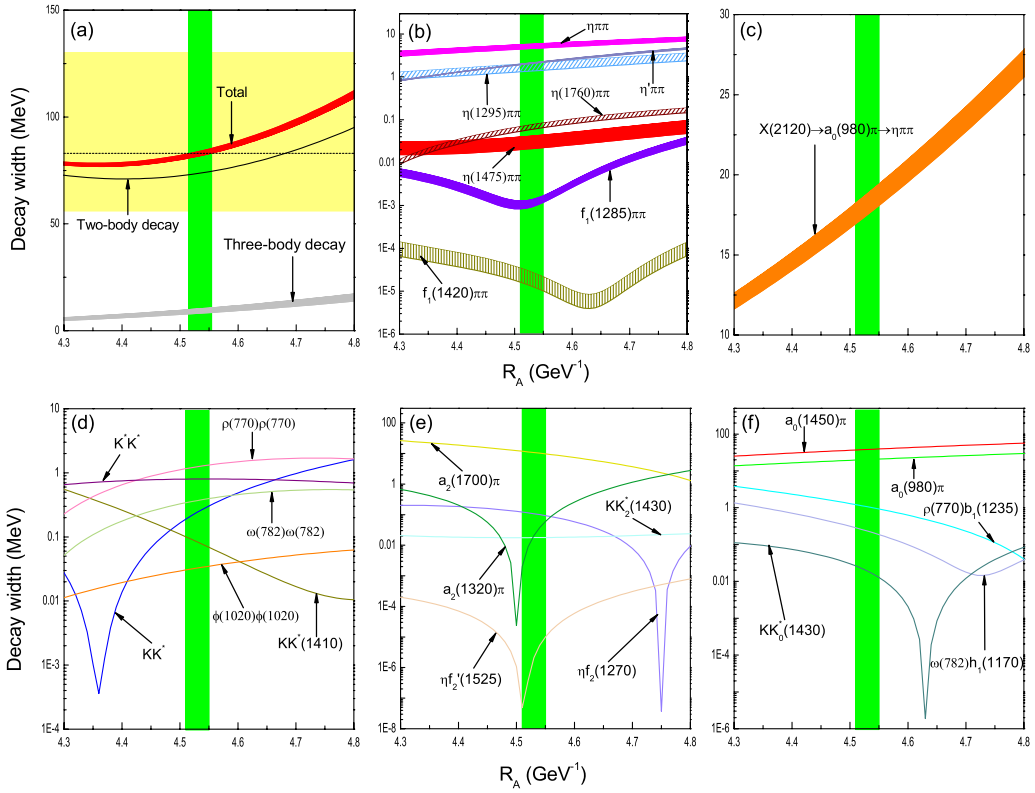

FIG. 9 (color online). The R dependence of the calculated total and partial widths of $X(2120)$ as the third radial excitation of $\eta(548)$. The partial widths presented in (a–c) are arranged in the same way as in Fig. 5, while the partial two-body decay widths are given in (d–f).

i.e., $\Gamma(\eta(1760) \to \rho(770)\rho(770)) = 41.3$–$42.7$ MeV, $\Gamma(\eta(1760) \to a_2(1320)\pi) = 21.8$–$22.3$ MeV, $\Gamma(\eta(1760) \to \omega(782)\omega(782)) = 15.0$–$14.6$ MeV, and $\Gamma(\eta(1760) \to a_0(980)\pi) = 10.6$–$10.8$ MeV.

BES-II and BES-III have given different widths (the dashed lines with yellow and blue bands) for $X(1835)$ as shown in Fig. 8(a). When comparing our calculation with the experimental width, we still adopt the resonance parameter from BES-II. It shows that the calculated decay width of $X(1835)$ under the assignment of the second radial excitation of $\eta'(958)$ is consistent with the BES-II measurement. The obtained R falls into 4.20–4.22 GeV^{-1}, which corresponds to the width of $X(1835)$ given by BES-II. This R value is quite close to that for $\eta(1760)$, and consistent with the estimate in Ref. [54]. The results presented in Fig. 8(d) further indicate that the decay widths of $X(1835)$ into $a_0(980)\pi$ and $a_0(1450)\pi$ can reach up to 24.5–25.2 MeV and 21.3–22.2 MeV, respectively.

The partial decay widths obtained by the QPC model seem to support the explanation for $\eta(1760)$ and $X(1835)$ as the second radial excitations of $\eta(548)$ and $\eta'(958)$. For the double pion decays, we find that the intermediate scalar productions appear to be the main contributor as shown in Figs. 7(b) and 8(b).

Because of $\eta\pi$ being the dominant decay channel of $a_0(980)$, in Figs. 7(c) and 8(c) the R dependence of the decay widths of $\eta(1760)/X(1835) \to a_0(980)\pi \to \eta\pi\pi$ also shows that contributions from intermediate a_0 productions are comparable with those via intermediate σ and $f_0(980)$ in $\eta(1760)/X(1835) \to \eta\pi\pi$. This prediction can be checked in future experiments.

C. $X(2120)$

The strong decay behaviors of $X(2120)$ are presented in Figs. 9 and 10. As shown in Fig. 9(a), the experimental width of $X(2120)$ can be reproduced by assuming $X(2120)$ as the third radial excitation of $\eta(548)$ with $R = 4.51$–4.55 GeV^{-1}. This range is also consistent with the R range estimated in Ref. [54]. The two-body partial decay widths of $X(2120)$ in Figs. 9(d)–9(f) indicate that $a_0(1450)\pi$, $a_0(980)\pi$, and $a_2(1700)\pi$ are the dominant decay channels, i.e., $\Gamma(X(2120) \to a_0(1450)\pi) = 37.6$–$40.1$ MeV, $\Gamma(X(2120) \to a_0(980)\pi) = 20.0$–$21.3$ MeV, and $\Gamma(X(2120) \to a_2(1700)\pi) = 9.2$–$11.3$ MeV. It should be noted that decays $X(2120) \to a_0(1450)\pi$, $a_0(980)\pi$ occur via S-wave while $X(2120) \to a_2(1700)\pi$ is via P-wave, which explains that the P-wave decay width is smaller than the S-wave.

The decay of $X(2120) \to a_0(980)\pi \to \eta\pi\pi$ occurs with considerable decay width due to the large coupling of $a_0(980) \to \eta\pi$. The results are shown in Fig. 9(c). Moreover, intermediate scalar states, i.e., σ and $f_0(980)$,

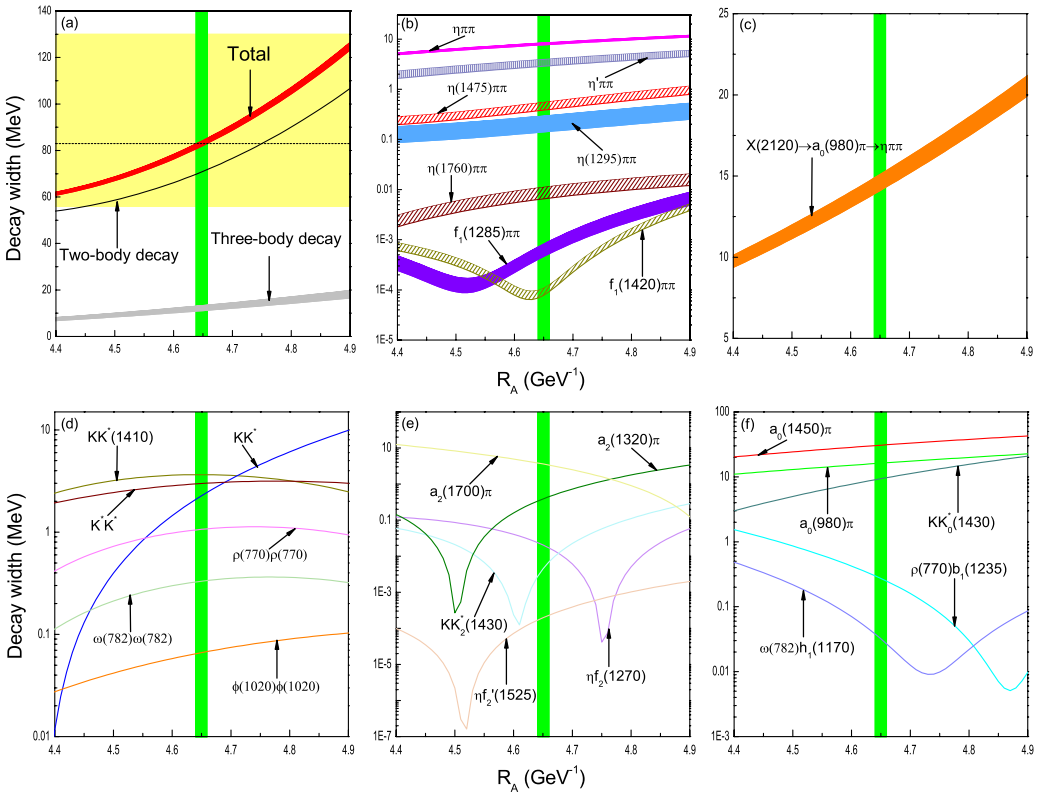

FIG. 10 (color online). The R dependence of the calculated total and partial widths of $X(2120)$ as the third radial excitation of $\eta(958)$. The partial widths presented in (a–c) are arranged in the same way as in Fig. 5, while the partial two-body decay widths are given in (d–f).

have also important contributions to the double pion decay channels, e.g., $X(2120) \to \eta\pi\pi$, $\eta'\pi\pi$. The results are presented in Fig. 9(b).

Under the assignment of the third radial excitation of $\eta'(958)$, one obtains the total decay width of $X(2120)$ [see Fig. 10(a)]. We can still find the overlap between theoretical and experimental total decay widths, with the obtained central values of $R = 4.64$–4.66 GeV^{-1}. This range is consistent with that for $X(2120)$ as the third radial excitation of $\eta(548)$. The results in Figs. 10(d)–10(f) show that $a_0(1450)\pi$ and $a_0(980)\pi$ are the main decay modes of $X(2120)$ if it is the third radial excitation of $\eta(958)$. This determines a sizeable decay width of $X(2120) \to a_0(980)\pi \to \eta\pi\pi$ [see Fig. 10(c)]. Again, we find important contributions from the intermediate scalar state in the double pion decays [see Fig. 10(b)]. The calculation suggests that both $\eta\pi\pi$ and $\eta'\pi\pi$ are important double pion decay modes of $X(2120)$.

Note that in Sec. II, the analysis of the mass spectrum of the $\eta - \eta'$ family indicates that there exists the partner of $X(2120)$ with the mass very close to that of $X(2120)$. Because of this, it is natural to set the mass of the partner of $X(2120)$ the same as 2.12 GeV. Thus, the above results should have reflected the theoretical expectations of the $X(2120)$ decay behavior as the third radial excitation of $\eta(548)$ or $\eta'(958)$.

D. $X(2370)$

In this subsection, we present the results for $X(2370)$ as the fourth radial excitation of $\eta(548)$ or $\eta'(958)$ in Figs. 11 and 12. Notice that more decay channels are open for $X(2370)$.

As the fourth radial excitation of $\eta(548)$, the obtained total decay width of $X(2370)$ is consistent with the experimental data [see Fig. 11(a)], where the central values of R are about 5 GeV^{-1}. The corresponding two-body decays indicate $X(2370)$ mainly decays into $a_0(980)\pi$, $a_0(980)\pi$, which are shown in Figs. 11(d)–11(h). In addition, KK^* and $a_2(1320)\pi$ channels also play an important role here. These implies the dominant contributions from intermediate scalars to the double pion decays of $X(2370) \to \eta\pi\pi$, $\eta'\pi\pi$, and $\eta(1295)\pi\pi$, as shown in Fig. 11(c).

If categorizing $X(2370)$ as the fourth radial excitation of $\eta'(958)$, one also obtains the total decay width of $X(2370)$ consistent with the experimental data with $R = 4.95$–4.96 GeV^{-1}. The comparison is shown in Fig. 12(a). The results in Figs. 12(d)–12(h) provide valuable information of main decay channels of $X(2370)$. Several main decay channels of $X(2370)$ include $a_0(1450)\pi$, KK^*, $KK_0^*(1430)$, $a_0(980)\pi$, $KK^*(1680)$, and $a_2(1320)\pi$. We list their partial decay

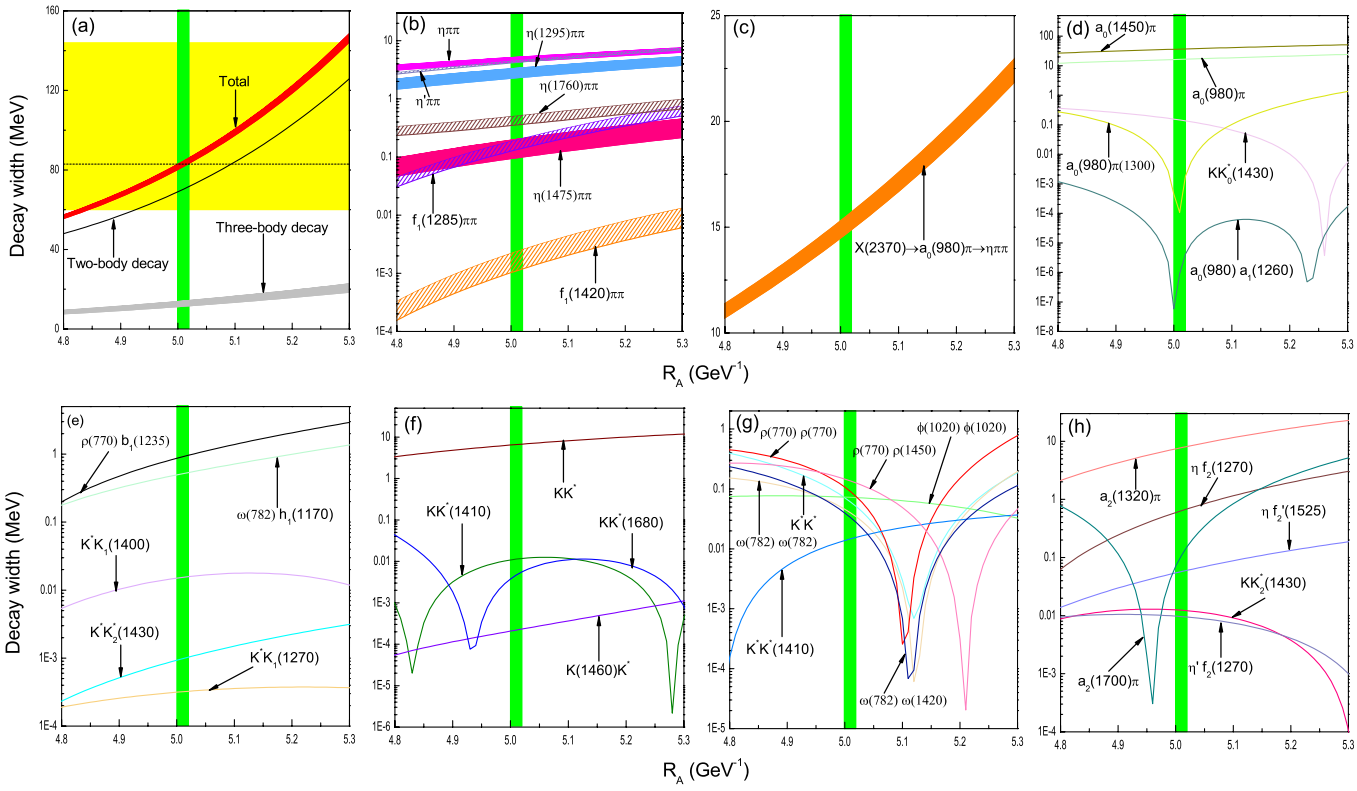

FIG. 11 (color online). The R dependence of the calculated total and partial widths of $X(2370)$ as the fourth radial excitation of $\eta(548)$. The partial widths presented in (a–c) are arranged in the same way as in Fig. 5, while the partial two-body decay widths are given in (d–f).

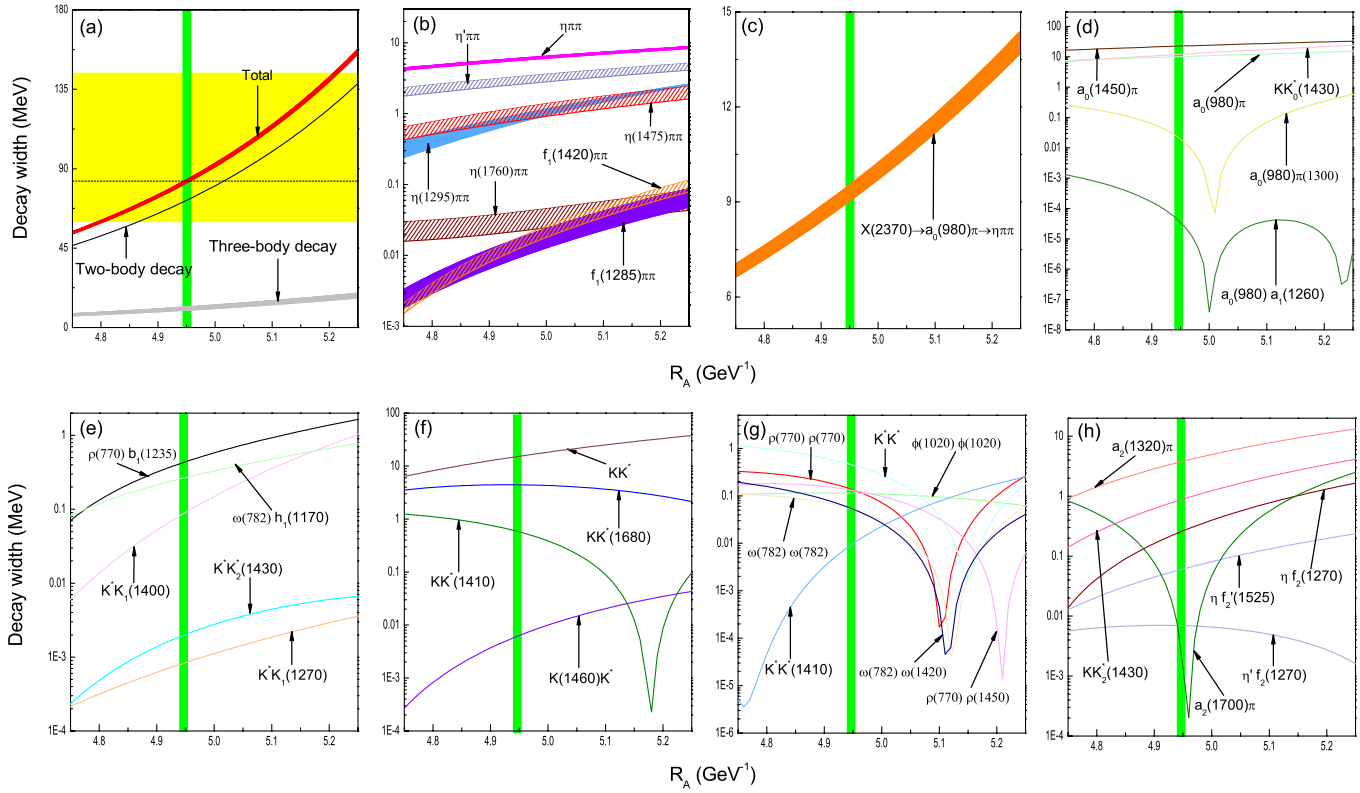

FIG. 12 (color online). The R dependence of the calculated total and partial widths of $X(2370)$ as the fourth radial excitation of $\eta(958)$. The partial widths presented in (a–c) are arranged in the same way as in Fig. 5, while the partial two-body decay widths are given in (d–f).

widths as a comparison: $\Gamma(X(2370) \to a_0(1450)\pi) = 22.6$–$22.9$ MeV, $\Gamma(X(2370) \to K^*K) = 15.4$–$15.9$ MeV, $\Gamma(X(2370) \to K^*K_0^*(1430)) = 12.2$–$12.5$ MeV, $\Gamma(X(2370) \to a_0(980)\pi) = 10.1$–$10.3$ MeV, $\Gamma(X(2370) \to K^*K^*(1680)) = 4.4$ MeV, and $\Gamma(X(2370) \to a_2(1320)\pi) = 3.8$–$4.0$ MeV. Again, it shows that the double pion decay widths will have important contributions from the intermediate scalars as shown in Fig. 12(b).

Note that $X(2370) \to KK_3^*(1780)$ is a F-wave decay, thus, will be suppressed in comparison with other low partial wave decays. In Figs. 11 and 12, we do not include the result of $X(2370) \to KK_3^*(1780)$.

We need to specify that the above numerical results are obtained by taking the mixing angle of $\eta(1295)/\eta(1475)$, $\eta(1760)/X(1835)$, $X(2120)$, and $X(2370)$ the same as the $\eta(548)/\eta'(958)$ mixing angle, i.e., $\theta_5 = \theta_4 = \theta_3 = \theta_2 = \theta_1 = 39.3°$. For further studying, the total decay widths of $\eta(1295)/\eta(1475)$, $\eta(1760)/X(1835)$, $X(2120)$, and $X(2370)$ dependent on θ_i and R, in Fig. 13, we present the 3D plot of the total decay widths of $\eta(1295)/\eta(1475)$, $\eta(1760)/X(1835)$, $X(2120)$, and $X(2370)$ with variables θ_i $(i = 1, \ldots, 5)$ and R. It would be useful for further constraining the theoretical calculations by experimental measurements.

V. DISCUSSION AND CONCLUSION

The confirmation of $X(1835)$ and observation of two new resonances, $X(2120)$ and $X(2370)$, by the BES-III Collaboration have inspired a lot efforts in the study of light hadron spectroscopy. In particular, it largely enriches our knowledge about the isoscalar and pseudoscalar spectrum. As stated earlier, $\pi(1300)$, $K(1460)$, $\eta(1295)$, and $\eta(1475)$ naturally make the first radial excitation states of 0^- mesons. Our speculation is that the second radial excitation nonet can be formed by $\pi(1800)$, $K(1830)$, $\eta(1760)$, and $X(1835)$. This categorizing scheme is in good agreement with the qualitative expectation of their mass spectrum in the constituent quark model. This scheme also allows us to accommodate $X(2120)$ and $X(2375)$ in the isoscalar pseudoscalar family as higher radial excitation states.

Within this categorizing scheme, we calculate the strong decay widths of these states in the QPC model to compare with the available experimental data. The results show that $\eta(1295)$, $\eta(1760)$ are good candidates of the first and the second radial excitations of $\eta(548)$, while $X(1835)$ can be explained as the second radial excitation of $\eta'(958)$. With a reasonable R range, the calculated total decay widths of $\eta(1295)$, $\eta(1760)$, $X(1835)$ agree well with the experimental data.

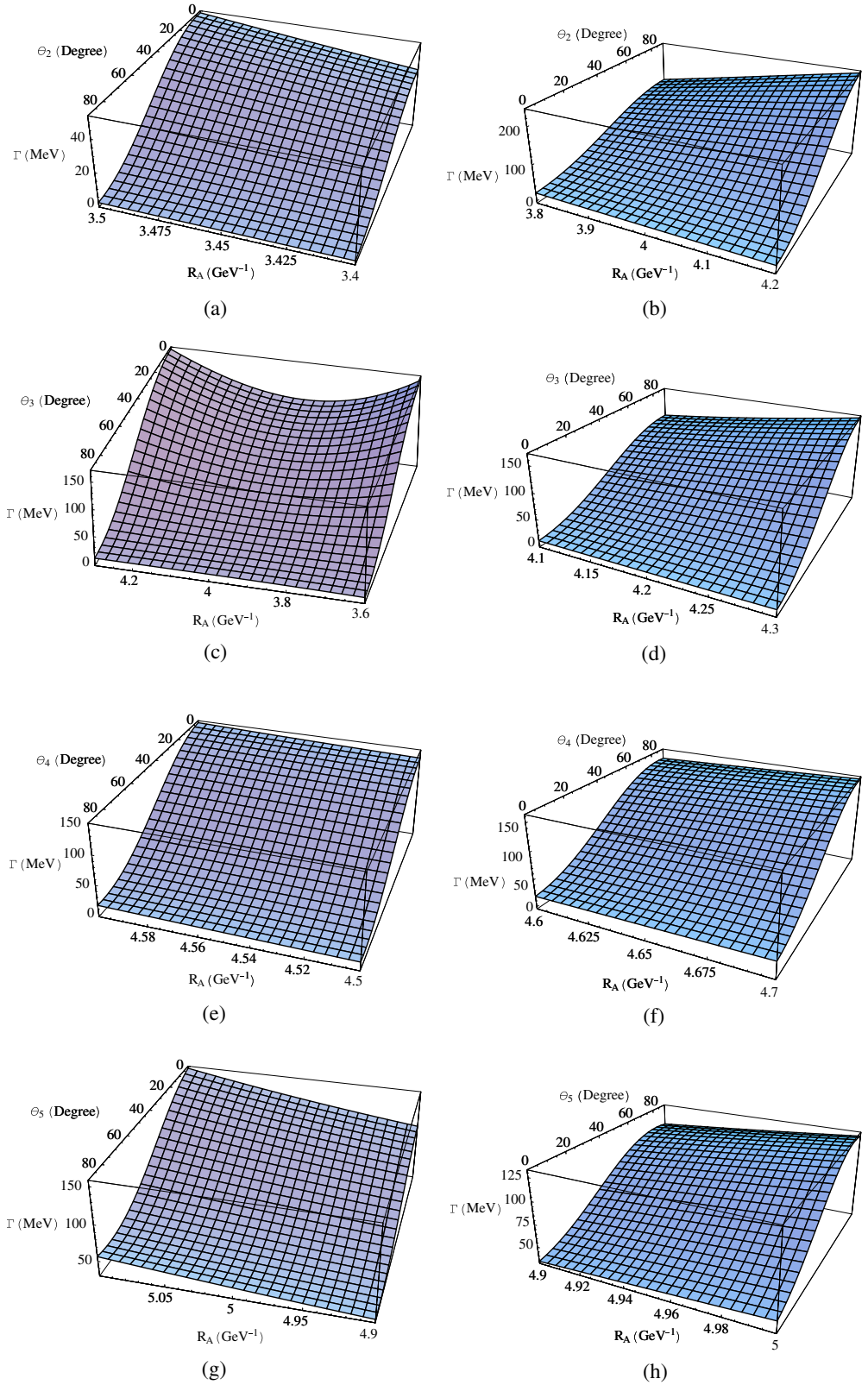

FIG. 13 (color online). The R and θ_i $(i = 2, \ldots, 5)$ dependence of the total decay widths of $\eta(1295)$, $\eta(1475)$, $\eta(1760)$, $X(1835)$, $X(2120)$, and $X(2370)$. (a), (b), (c), and (d) correspond to the decays of $\eta(1295)$, $\eta(1475)$, $\eta(1760)$, and $X(1835)$, respectively. Diagrams (e)/(f) show the decay behaviors of $X(2120)$ as the third radial excitation of $\eta(548)/\eta'(958)$, while the variation of the decay behaviors of $X(2370)$ to θ_5 and R is given in diagrams (g)/(h) with $X(2370)$ as the fourth radial excitation of $\eta(548)/\eta'(958)$.

For $\eta(1475)$, the R range is larger than that for $\eta(1295)$ if one requires the calculated width to fit the experimental data well. Under such a condition, the decay mode $a_0(98)\pi$ becomes the main contributor to the total width for $\eta(1475)$, which, however, does not coincide with the experimental observation since $\eta(1475)$ mainly decays into $K\bar{K}\pi$. By assigning $\eta(1475)$ as the partner of $\eta(1295)$, and thus its R range being the same as that of $\eta(1295)$, we find that the decay width of $K\bar{K}^* + c.c.$ becomes comparable with that of $a_0(980)\pi$. The dominance of the $K\bar{K}\pi$ decay mode can be recovered. It is likely that the total width of $\eta(1475)$ was overestimated by experiment due to large uncertainties. Therefore, more precise data for the $\eta(1475)$ resonance parameters are strongly recommended in future experiments.

Our calculation suggests that $X(2120)$ and $X(2370)$ could be as the third and fourth radial excitations of $\eta(548)/\eta'(958)$, respectively. Since the masses of the partners of the same radial excitations are close to each other, we analyze both possibilities and predict their strong decay patterns. It should be useful for experimental search for their partners in other channels such as $\eta\pi\pi$ and $K\bar{K}\pi$.

It is interesting to note that apart from those three enhancements, $X(1835)$, $X(2120)$, and $X(2370)$, an enhancement around 1.5 GeV also appears in the $\eta'\pi\pi$ invariant spectrum [1]. A possible assignment to $f_1(1510)$ was discussed in Ref. [1]. We notice that a pseudoscalar state $\eta(1475)$ would be favored by an S-wave decay into $\eta'\pi\pi$, while $f_1(1510) \to \eta'\pi\pi$ would be via a P-wave. Our calculation shows that $\eta(1475)$ should have a sizeable contribution to the $\eta'\pi\pi$ invariant mass spectrum. The slight mass shift could be due to its interferences with other contributions. Thus, to make sure whether there is $\eta(1475)$ contribution in the $\eta'\pi^+\pi^-$ mode, a partial wave analysis with $\eta(1475)$ included in the fit should be tested. We also mention that, as the second radial excitation of $\eta(548)$, the dominant double pion decay channel of $\eta(1760)$ is via $\eta(1760) \to \eta\pi\pi$ instead of $\eta(1760) \to \eta'\pi\pi$. Therefore, it may not appear predominant in the $\eta'\pi\pi$ invariant mass spectrum. It should also be recognized that the inclusion of $\eta(1760)$ will have important interfering effects with other resonance amplitudes, which could be essential for extracting the resonance parameters in the partial wave analysis. We expect that the future partial wave analysis from BES-III can testify this point.

To summarize, the new data from BES-III have provided important information on the pseudoscalar spectrum, and could be so far, the first observation of higher radial excitations of η/η' states. It will greatly enrich our knowledge about the light hadron spectrum, and will be useful for further efforts on the study of exotic states in both experiment and theory. We expect that more experimental data from BES-III in the near future will bring great opportunities for our understanding of the strong QCD in the light hadron sector.

ACKNOWLEDGMENTS

We would like thank Shan Jin, Xue-Qian Li, Hai-Yang Cheng, Dian-Yong Chen, Jun He, Bin Chen, and D. V. Bugg for useful discussions. This project is supported in part by the National Natural Science Foundation of China (Grants No. 11035006, No. 11047606, No. 11035006), the Ministry of Education of China (FANEDD under Grant No. 200924, DPFIHE under Grant No. 20090211120029, NCET under Grant No. NCET-10-0442, the Fundamental Research Funds for the Central Universities under Grant No. lzujbky-2010-69), and the Chinese Academy of Sciences (KJCX2-EW-N01).

[1] M. Ablikim *et al.* (BESIII Collaboration), Phys. Rev. Lett. **106**, 072002 (2011).
[2] M. Ablikim *et al.* (BES Collaboration), Phys. Rev. Lett. **95**, 262001 (2005).
[3] N. Kochelev and D. P. Min, Phys. Lett. B **633**, 283 (2006).
[4] N. Kochelev and D. P. Min, Phys. Rev. D **72**, 097502 (2005).
[5] X. G. He, X. Q. Li, X. Liu, and J. P. Ma, Eur. Phys. J. C **49**, 731 (2006).
[6] B. A. Li, Phys. Rev. D **74**, 034019 (2006).
[7] G. Hao, C. F. Qiao, and A. L. Zhang, Phys. Lett. B **642**, 53 (2006).
[8] J. Z. Bai *et al.* (BES Collaboration), Phys. Rev. Lett. **91**, 022001 (2003).
[9] A. Datta and P. J. O'Donnell, Phys. Lett. B **567**, 273 (2003).
[10] C. S. Gao and S. L. Zhu, Commun. Theor. Phys. **42**, 844 (2004).
[11] M. L. Yan, S. Li, B. Wu, and B. Q. Ma, Phys. Rev. D **72**, 034027 (2005).
[12] X. Liu, X. Q. Zeng, Y. B. Ding, X. Q. Li, H. Shen, and P. N. Shen, arXiv:hep-ph/0406118.
[13] M. Ablikim *et al.* (BESIII Collaboration), arXiv:1001.5328.
[14] J. P. Alexander *et al.* (CLEO Collaboration), Phys. Rev. D **82**, 092002 (2010).
[15] G. J. Ding and M. L. Yan, Eur. Phys. J. A **28**, 351 (2006).
[16] M. L. Yan, arXiv:hep-ph/0605303.
[17] G. J. Ding and M. L. Yan, Phys. Rev. C **75**, 034004 (2007).
[18] Z. G. Wang and S. L. Wan, J. Phys. G **34**, 505 (2007).
[19] C. Liu, Eur. Phys. J. C **53**, 413 (2007).
[20] J. P. Dedonder, B. Loiseau, B. El-Bennich, and S. Wycech, Phys. Rev. C **80**, 045207 (2009).
[21] Y. L. Ma, J. Phys. G **36**, 055004 (2009).
[22] T. Huang and S. L. Zhu, Phys. Rev. D **73**, 014023 (2006).

[23] D. M. Li and B. Ma, Phys. Rev. D **77**, 074004 (2008).
[24] C. Amsler *et al.* (Particle Data Group), Phys. Lett. B **667**, 1 (2008).
[25] E. Klempt and A. Zaitsev, Phys. Rep. **454**, 1 (2007).
[26] A. Masoni, C. Cicalo, and G. L. Usai, J. Phys. G **32**, R293 (2006).
[27] D. V. Bugg, arXiv:1101.1642.
[28] S. B. Gerasimov, M. Majewski, and V. A. Meshcheryakov, J. Phys. G **38**, 035008 (2011).
[29] H. Y. Cheng, H. N. Li, and K. F. Liu, Phys. Rev. D **79**, 014024 (2009).
[30] T. Gutsche, V. E. Lyubovitskij, and M. C. Tichy, Phys. Rev. D **80**, 014014 (2009).
[31] F. E. Close, G. R.Farrar, and Z. Li, Phys. Rev. D **55**, 5749 (1997).
[32] D. M. Li, H. Yu, and S. S. Fang, Eur. Phys. J. C **28**, 335 (2003).
[33] G. Li, Q. Zhao, and C.-H. Chang, J. Phys. G **35**, 055002 (2008).
[34] L. Faddeev, A. J. Niemi, and U. Wiedner, Phys. Rev. D **70**, 114033 (2004).
[35] M. Ablikim *et al.* (Bes Collaboration), Phys. Rev. D **73**, 112007 (2006).
[36] D. Bisello *et al.* (DM2 Collaboration), Phys. Rev. D **39**, 701 (1989).
[37] G. F. Chew and S. C. Frautschi, Phys. Rev. Lett. **8**, 41 (1962).
[38] A. V. Anisovich, V. V. Anisovich, and A. V. Sarantsev, Phys. Rev. D **62**, 051502 (2000).
[39] J. F. Liu, G. J. Ding, and M. L. Yan, Phys. Rev. D **82**, 074026 (2010).
[40] L. Micu, Nucl. Phys. **B10**, 521 (1969).
[41] A. Le Yaouanc, L. Oliver, O. Pène, and J. Raynal, Phys. Rev. D **8**, 2223 (1973); **9**, 1415 (1974); **11**, 1272 (1975); Phys. Lett. **72B**, 57 (1977); **71B**, 397 (1977).
[42] A. Le Yaouanc, L. Oliver, O. Pene, and J. C. Raynal, Phys. Lett. **72B**, 57 (1977).
[43] A. Le Yaouanc, L. Oliver, O. Pene, and J. C. Raynal, *Hadron Transitions in the Quark Model* (Gordon and Breach, New York, 1988), p. 311.
[44] E. van Beveren, C. Dullemond, and G. Rupp, Phys. Rev. D **21**, 772 (1980); **22**, 787(E) (1980); E. van Beveren, G. Rupp, T. A. Rijken, and C. Dullemond, Phys. Rev. D **27**, 1527 (1983).
[45] R. Bonnaz, B. Silvestre-Brac, and C. Gignoux, Eur. Phys. J. A **13**, 363 (2002).
[46] W. Roberts and B. Silvestre-Brac, Few-Body Syst. **11**, 171 (1992).
[47] H. G. Blundell and S. Godfrey, Phys. Rev. D **53**, 3700 (1996).
[48] P. R. Page, Nucl. Phys. **B446**, 189 (1995).
[49] S. Capstick and N. Isgur, Phys. Rev. D **34**, 2809 (1986).
[50] S. Capstick and W. Roberts, Phys. Rev. D **49**, 4570 (1994).
[51] E. S. Ackleh, T. Barnes, and E. S. Swanson, Phys. Rev. D **54**, 6811 (1996).
[52] H. Q. Zhou, R. G. Ping, and B. S. Zou, Phys. Lett. B **611**, 123 (2005).
[53] X. H. Guo, H. W. Ke, X. Q. Li, X. Liu, and S. M. Zhao, Commun. Theor. Phys. **48**, 509 (2007).
[54] F. E. Close and E. S. Swanson, Phys. Rev. D **72**, 094004 (2005).
[55] J. Lu, W. Z. Deng, X. L. Chen, and S. L. Zhu, Phys. Rev. D **73**, 054012 (2006).
[56] B. Zhang, X. Liu, W. Z. Deng, and S. L. Zhu, Eur. Phys. J. C **50**, 617 (2007).
[57] C. Chen, X. L. Chen, X. Liu, W. Z. Deng, and S. L. Zhu, Phys. Rev. D **75**, 094017 (2007); X. Liu, C. Chen, W. Z. Deng, and X. L. Chen, Chinese Phys. C **32**, 424 (2008).
[58] Z. F. Sun and X. Liu, Phys. Rev. D **80**, 074037 (2009).
[59] X. Liu, Z. G. Luo, and Z. F. Sun, Phys. Rev. Lett. **104**, 122001 (2010).
[60] Z. F. Sun, J. S. Yu, X. Liu, and T. Matsuki, Phys. Rev. D **82**, 111501 (2010).
[61] D. M. Li and B. Ma, Phys. Rev. D **77**, 094021 (2008); D. M. Li and S. Zhou, Phys. Rev. D **78**, 054013 (2008); Phys. Rev. D **79**, 014014 (2009).
[62] Z. G. Luo, X. L. Chen, and X. Liu, Phys. Rev. D **79**, 074020 (2009).
[63] M. Jacob and G. C. Wick, Ann. Phys. (N.Y.) **7**, 404 (1959); **281**, 774 (2000).
[64] T. Feldmann, P. Kroll, and B. Stech, Phys. Rev. D **58**, 114006 (1998).
[65] H. Y. Cheng, Phys. Rev. D **67**, 034024 (2003).
[66] A. V. Anisovich, V. V. Anisovich, and V. A. Nikonov, Eur. Phys. J. A **12**, 103 (2001).
[67] D. M. Li, B. Ma, and H. Yu, Eur. Phys. J. A **26**, 141 (2005).
[68] L. S. Geng, F. K. Guo, C. Hanhart, R. Molina, E. Oset, and B. S. Zou, Eur. Phys. J. A **44**, 305 (2010).
[69] D. M. Li, H. Yu, and Q. X. Shen, J. Phys. G **27**, 807 (2001).
[70] M. Kirchbach and D. O. Riska, Nucl. Phys. **A594**, 419 (1995).
[71] H. Hatanaka and K. C. Yang, Phys. Rev. D **77**, 094023 (2008); **78**, 059902(E) (2008).
[72] Z. Bai *et al.* (MARK-III Collaboration), Phys. Rev. Lett. **65**, 2507 (1990).